Quantum effects in the giant magnetoresistance of magnetic multilayered structures

1993 J. Phys.: Condens. Matter 5 8289

(http://iopscience.iop.org/0953-8984/5/44/019)

J. Phys.: Condens. Matter 5 (1993) 8289–8304. Printed in the UK

Quantum effects in the giant magnetoresistance of magnetic multilayered structures

A Vedyayev†, C Cowache, N Ryzhanova‡ and B Dieny

CEA Département de Recherche Fondamentale sur la Matière Condensée, CENG, SP2M/MP, 85X, 38041 Grenoble Cédex, France

Received 8 June 1993, in final form 2 August 1993

Abstract. We present an analytical quantum statistical theory of giant magnetoresistance in magnetic multilayers (current flowing in the plane of the layers) which takes into account both spin-dependent scattering of conduction electrons (s, d or hybridized sd electrons) and spin-dependent potential barriers between successive layers. The model also includes quantization of the momentum of conduction electrons in the direction perpendicular to the plane of the layers (k_z). The influence of the following parameters is discussed: ratio of spin-up to spin-down mean free paths, height of potential barriers between adjacent materials and thicknesses of the various layers. It is shown that the main contribution to the giant magnetoresistance is spin-dependent scattering rather than spin-dependent potential barriers. In fact, if the mean free paths of spin-up and spin-down electrons in the magnetic material are significantly different, the presence of potential barriers (spin-dependent or not) can only decrease the magnetoresistance amplitude. Furthermore, the quantization of component momentum k_z leads to well-defined oscillations of magnetoresistance with respect to thicknesses of the various layers. It should be possible to observe these quantum oscillations experimentally.

1. Introduction

The discovery of giant magnetoresistance effects in the Fe/Cr superlattice [1] triggered a large number of studies on the transport properties of magnetic multilayers and sandwiches. Since 1988 this effect has been observed in a large variety of magnetically-coupled multilayers (where successive magnetic layers are coupled antiferromagnetically through a paramagnetic spacer layer [2–4]) or in magnetic sandwiches (where magnetic layers have different coercitivities or are coupled by exchange anisotropy to other layers [5–8]). In both types of system, it is possible to change the relative orientation of magnetization in the successive ferromagnetic layers—from antiparallel to parallel or vice versa—by applying an external magnetic field. This change from a configuration of parallel magnetizations to a configuration of antiparallel magnetizations is at the origin of so-called giant magnetoresistance (GMR). It is now widely admitted that the underlying mechanism of GMR is a coherent interplay, between successive ferromagnetic layers, of spin-dependent scattering (SDS) of conduction electrons occurring at the interfaces or in the bulk of the magnetic layers [1, 9–19]. More generally, GMR is related to the difference of microscopic

† Permanent address: Department of Physics, Moscow Lomonosov University, Moscow, 119899, Russia.

‡ Permanent address: I.V.P., Modus, Moscow, 119899, Russia.

0953-8984/93/448289+16$07.50

electronic properties of spin-up and spin-down electrons' subsystems in ferromagnetic metals and to the non-local character of the conductivity $\sigma(Z, Z')$ in the relation

$$j(Z) = \int \sigma(Z, Z')E(Z')\,d^3Z'$$

where $j(Z)$ is the current density at point Z and $E(Z')$ the electrical field at point Z'.

Theories of GMR [9–21] based on spin-dependent scattering of conduction electrons have been developed using two main different approaches:

(i) quasi-classical, based on Boltzmann equation and Fuchs–Sondheimer theory for size effects in electronic transport [9–14];

(ii) quantum-statistical, based on Kubo formalism [15–18].

A detailed comparison of these different approaches has been made in [20] and [21]. It was shown that they are almost equivalent under the condition of applicability of quasi-classical approach itself; i.e. if it is possible:

(i) to neglect the quantization of electron momentum due to the finite size of the samples in the direction perpendicular to the layers. The corresponding condition is $k_F L \gg 1$ (k_F =Fermi momentum and L =period or total thickness of the multilayer, depending on the modulation of the lattice potential).

(ii) to neglect quantum interference effects. This requires $k_F \mathcal{L} \gg 1$ ($\mathcal{L}$ =electron mean free path).

Furthermore, in most of these theories (except [14] and [17]) the influence of potential barriers between successive layers has not been taken into account (assumption of free electron gas with flat potential).

In this paper, we develop a quantum theory of GMR in magnetic multilayers of period (ferromagnetic transition metal/non-magnetic transition or noble metal) which in addition to the spin-dependent scattering in the multilayers also includes the quantization of electron momentum in the direction perpendicular to the plane of the layers and the existence of potential barriers associated with the chemical modulation of the multilayers [14]. The question of the influence of potential barriers between adjacent layers is intimately related to the nature of the electrons which carry the current in transition metals (sp, d electrons and/or hybridized electrons). It may be argued that sp electrons carry most of the current, because of their generally low effective mass [22]. For these electrons, the potential barrier between two adjacent layers corresponds to the difference in energy between the bottom of the sp band and Fermi energy in the two materials considered. Consequently, their height is of the order of a few tenths of an eV to be compared with the few eV for Fermi energy [23]: even if the barriers are usually small for sp electrons (of the order of 10% of Fermi energy ϵ_F), they are not always negligible. Another point is that exchange splitting of the sp band in ferromagnetic transition metals is quite small compared to the Fermi energy; this implies that the barriers are not or are only very weakly spin-dependent for sp electrons.

However, it has been pointed out that d electrons in ferromagnetic transition metals can also have quite a significant contribution to the conduction of the current [24]. For these electrons, the scattering asymmetry is generally larger because of a significant difference in density of states at ϵ_F between the d-spin-up and d-spin-down subbands. Moreover, the height of the potential barriers can be fairly large—even comparable to the Fermi energy—and is strongly spin-dependent because of the d-band splitting in transition metals.

Consequently, and in order to describe more accurately the transport properties in transition metal based multilayers, it is important to take into account both the spin-dependent scattering cross-section of conduction electrons and the spin-dependent modulation of the lattice potential throughout the multilayer.

2. Model

We consider the case of a sandwich consisting of two ferromagnetic transition-metal layers F1 and F2 separated by a non-magnetic spacer NM. Such sandwich is labelled (F1a/NM b/F2 c) in which a, b and c refer to the thickness of the respective layers. The electric current flows in the plane of the sample and electron motion is constrained by infinite potential walls at the outer surfaces of the sandwich. As discussed in [17], this situation is equivalent to the case of an infinite multilayer of period (F1 $2a$/NM b/F2 $2c$/NM b).

We suppose that we are able to change the magnetic configuration of the sample (from antiparallel to parallel or vice versa) by applying an external magnetic field. The conductivity for both alignments of magnetizations is obtained by adding the contributions of spin-up and spin-down electrons calculated separately. This is the two-current model which provides a good description of electron transport in magnetic transition metals (spin-flip processes can be neglected in 3d transition metals at low temperature). Electrons are considered as 'free', with spherical Fermi surfaces. Within each layer, they move in a constant potential which depends on the layer and on their spin. The Fermi momentum $k_F^{\uparrow(\downarrow)}$ is related to the Fermi energy ϵ_F via the relation: $k_F^{\uparrow(\downarrow)} = (1/\hbar)\sqrt{2m(\epsilon_F - U^{\uparrow(\downarrow)})}$ in which m represents the effective mass of electrons and $(\epsilon_F - U^{\uparrow(\downarrow)})$ the difference between the Fermi energy and the bottom of the conduction band for spin-up or spin-down electrons. There is therefore a direct relationship between potential barrier height and difference in Fermi momenta between adjacent magnetic and non-magnetic materials. Consequently, in what follows, we discuss the influence of potential barriers in terms of differences in Fermi momenta rather than differences in potential. Furthermore, the number of electrons of each species (spin-up or spin-down) per unit volume ($n^{\uparrow(\downarrow)}$) varies with $k_F^{\uparrow(\downarrow)}$ according to $n^{\uparrow(\downarrow)} = k_F^{\uparrow(\downarrow)3}/6\pi^2$.

As we are investigating the case in which mean free paths and Fermi momenta are spin dependent, we write down the Hamiltonian of our system as a generalization of the sd model for ferromagnetic binary alloys $A_{1-x}B_x$ developed in [25]. A and B are the two components of the alloy, and $1-x$ and x their atomic concentrations. In the case of Permalloy, A and B represent respectively Ni and Fe; in the case of a pure transition metal, B represents the impurities which provoke the scattering of electrons. The Hamiltonian is written

$$\hat{H} = \sum_k E_s(k)|k_s^\sigma\rangle\langle k_s^\sigma| + \sum_k E_d(k)|k_d^\sigma\rangle\langle k_d^\sigma| + \sum_n \epsilon_{d,\mu}^{n,\sigma}|n_d^\sigma\rangle\langle n_d^\sigma| + \sum_k \gamma(|k_s^\sigma\rangle\langle k_d^\sigma| + |k_d^\sigma\rangle\langle k_s^\sigma|). \tag{1}$$

In this expression, the two first terms represent the total kinetic energies of s and d electrons respectively, the third term the scattering of d electrons and the fourth term the sd hybridization. The scattering of s electrons is not explicitly introduced as it is for d electrons but is nevertheless taken into account via sd hybridization. $E_d(k)$ and $E_s(k)$ are the kinetic energies for d and s electrons; $|k_s^\sigma\rangle$, $\langle k_s^\sigma|$, $|k_d^\sigma\rangle$ and $\langle k_d^\sigma|$ are the annihilation–creation operators for Bloch states; $|n_d^\sigma\rangle$ and $\langle n_d^\sigma|$ are the annihilation–creation operators for Wannier states; γ is the hybridization constant; $\epsilon_{d,\mu}^{n,\sigma}$ is the position of the d level, depending on the spin index $\sigma(+/-1)$ through exchange splitting and taking the value $\epsilon_{d,\mu}^{A,\sigma}$ or $\epsilon_{d,\mu}^{B,\sigma}$ with the probability x^μ and $1-x^\mu$ respectively; and μ is the index relative to the layer (1 and 3 for the two ferromagnetic layers, 2 for the paramagnetic spacer).

To proceed further we have to calculate retarded and advanced Green functions of the Hamiltonian (1). These Green functions are averaged at a microscopic scale over the

distribution of A and B atoms within each layer. Nonetheless they remain inhomogeneous at the scale of the layers' thicknesses. To carry out this calculation, it is convenient to use mixed (K, Z) representation [17], where K is the component of electron momentum in the plane of the film and Z the coordinate perpendicular to the plane. The coherent potential approximation (CPA) is used to average the Green functions at the microscopic scale.

Spin-dependent coherent potentials for d electrons within each layer ($\Sigma^{\sigma}_{d\mu}(E)$) are determined by the following equation:

$$\Sigma^{\sigma}_{d\mu}(E) = \bar{\epsilon}_{d\mu} + \frac{x^{\mu}(1-x^{\mu})(\epsilon^{A,\sigma}_{d,\mu} - \epsilon^{B,\sigma}_{d,\mu})F^{\sigma}_{dd,\mu}(E)}{1 + (\bar{\epsilon}_{d\mu} + \Sigma^{\sigma}_{d\mu}(E))F^{\sigma}_{dd,\mu}(E)} \tag{2}$$

where $\bar{\epsilon}_{d\mu} = x^{\mu}\epsilon^{A,\sigma}_{d,\mu} + (1-x^{\mu})\epsilon^{B,\sigma}_{d,\mu}$ represents the average potential energy in layer μ and $F^{\sigma}_{dd,\mu}(E)$ is the diagonal dd part of the Green function in layer μ for electrons with spin σ.

As a first step in the self-consistent calculation of the coherent potentials and of the Green functions, we use for the expression $F^{\sigma}_{dd,\mu}(E)$ the relation

$$F^{\sigma}_{dd,\mu}(E) = \int d\epsilon \frac{\rho_{os}(\epsilon)}{E - \Sigma^{\sigma}_{d\mu}(E) - \alpha\epsilon - \gamma^2(E-\epsilon)^{-1}}$$

established for bulk materials [25]. In this formula, α is the ratio of d-band to s-band widths and $\rho_{os}(\epsilon)$ is the density of s-electron states in the pure metal, neglecting sd hybridization.

For s electrons, the effective coherent potentials $\Sigma^{\sigma}_{s\mu}(E)$ may be approximated as:

$$\Sigma^{\sigma}_{s\mu}(E) \approx \frac{\gamma^2}{E - \Sigma^{\sigma}_{d\mu}} \approx \gamma^2(\mathrm{Re}[F^{\sigma}_{dd,\mu}(E)] \mp \mathrm{Im}[F^{\sigma}_{dd,\mu}(E)])$$

where $(1/\pi)\mathrm{Im}[F^{\sigma}_{dd,\mu}(E)]$ is the density of d-electron states with spin σ. In ferromagnetic transition metals, the density of d states for spin-up and spin-down electrons can be rather large near ϵ_F and quite different for the two species of electrons [23]. As a consequence, the ratio of mean free paths for spin-up and spin-down electrons may also be very large (or small). This situation is quite different from that in [15] in which the ratio of mean free paths is proportional to the quantity $|(\omega - j)/(\omega + j)|^2$ (where ω is the scattering impurity potential and j that of the sd-exchange integral). Indeed, j is usually much smaller than ω so in this model the ratio of mean free paths cannot be very different from one.

3. Green functions, conductivity and magnetoresistance

To make the situation more tractable, we now consider s and d electrons separately, choosing the values of $\Sigma^{\sigma}_{s\mu}$ and $\Sigma^{\sigma}_{d\mu}$ as effective potentials for s and d electrons. Besides that, we neglect the discreteness of the lattice.

Within these assumptions, the Green functions for s and d electrons are solutions of the equation:

$$\left(E - \frac{\hbar^2K^2}{2m} + \frac{\hbar^2}{2m}\frac{\partial^2}{\partial z^2} - \Sigma^{\sigma}_{\mu}\right)G(Z, Z') = a_0\delta(Z - Z') \tag{3}$$

with boundary conditions $G(Z'+\epsilon, Z') = G(Z'-\epsilon, Z')$ and

$$\left.\frac{\partial G}{\partial Z}\right|_{Z=Z'+\epsilon} - \left.\frac{\partial G}{\partial Z}\right|_{Z=Z'-\epsilon} = a_0\frac{2m}{\hbar^2}$$

when $\epsilon \to 0$. Also, $G(Z, Z') = 0$ on outer boundaries (for $Z, Z' = 0$ or $a + b + c$), $G(a + \epsilon, Z') = G(a - \epsilon, Z')$, $G(a + b + \epsilon, Z') = G(a + b - \epsilon, Z')$ and corresponding equalities for derivatives at inner boundaries.

Equation (3) is exactly the same as in [17], but here it is solved exactly without the restriction $|\Sigma_\mu^\sigma/\epsilon_F| \ll 1$.

As mentioned in the preceding section, in order to make the calculation completely self-consistent, we should calculate the coherent potentials Σ_μ^σ from equation (2) in which $F_{dd,\mu}^\sigma(E)$ would be the diagonal dd part of the Green function calculated from equation (3) which depends itself on Σ_μ^σ. Our approximation which uses for $F_{dd,\mu}^\sigma(E)$ the expression for the bulk material is the first step in this iterative self-consistent calculation. This approximation is valid as long as thicknesses are large compared to k_F^{-1} and differences of potentials $|\Sigma_{\mu_i}^{\pm\sigma} - \Sigma_{\mu_j}^{\pm\sigma}|$ are small compared to ϵ_F.

For the Green functions, we then get the following expressions:

(i)

$$G(Z, Z') = -\frac{2ma_0}{\hbar^2\kappa_1}\frac{\sin\kappa_1 Z}{\text{Den}}\left\{\begin{array}{l}\kappa_1\cos\kappa_1(Z-a)\left[\dfrac{\kappa_3}{\kappa_2}\cos\kappa_3 c\sin\kappa_2 b + \cos\kappa_2 b\sin\kappa_3 c\right] \\ -\kappa_2\sin\kappa_1(Z-a)\left[\dfrac{\kappa_3}{\kappa_2}\cos\kappa_3 c\cos\kappa_2 b - \sin\kappa_3 c\sin\kappa_2 b\right]\end{array}\right\}$$

when Z and $Z' \in [a]$ and $Z > Z'$; the notation $Z \in [a]$ means that the coordinate Z corresponds to a position along the z-axis within the layer of thickness a.

(ii)

$$G(Z, Z') = -\frac{2ma_0}{\hbar^2\kappa_2}\frac{1}{\text{Den}}\left\{\begin{array}{l}[\kappa_2\cos\kappa_2(Z-a-b)\sin\kappa_3 c - \kappa_3\sin\kappa_2(Z-a-b)\cos\kappa_3 c] \\ -[\kappa_2\cos\kappa_2(Z'-a)\sin\kappa_1 a - \kappa_3\sin\kappa_2(Z'-a)\cos\kappa_1 a]\end{array}\right\}$$

when Z and $Z' \in [b]$ and $Z > Z'$.

(iii)

$$G(Z, Z') = \frac{2ma_0}{\hbar^2\kappa_2}\frac{\sin\kappa_3(Z'-D)}{\text{Den}} \times \left\{\begin{array}{l}\kappa_3\cos\kappa_3(Z-a-b)\left[\dfrac{\kappa_1}{\kappa_2}\cos\kappa_1 a\sin\kappa_2 b + \cos\kappa_2 b\sin\kappa_1 a\right] \\ -\kappa_1\sin\kappa_3(Z-a-b)\left[\dfrac{\kappa_2}{\kappa_1}\sin\kappa_1 a\sin\kappa_2 b - \cos\kappa_1 a\cos\kappa_2 b\right]\end{array}\right\}$$

when Z and $Z' \in [c]$ and $Z < Z'$.

(iv)

$$G(Z, Z') = -\frac{2ma_0}{\hbar^2\kappa_2}\frac{\sin\kappa_1 Z}{\text{Den}}[\kappa_2\cos\kappa_2(Z'-a-b)\sin\kappa_3 c - \kappa_3\sin\kappa_2(Z'-a-b)\cos\kappa_3 c]$$

when $Z \in [a]$ and $Z' \in [b]$.

(v)

$$G(Z, Z') = \frac{2ma_0}{\hbar^2\kappa_2}\frac{\sin\kappa_1 Z'\sin\kappa_3(Z-D)}{\text{Den}}$$

when $Z \in [c]$ and $Z' \in [a]$.

(vi)

$$G(Z, Z') = \frac{2ma_0}{\hbar^2\kappa_2}\frac{\sin\kappa_3(Z-D)}{\text{Den}}[\kappa_2\cos\kappa_2(Z'-a)\sin\kappa_1 a + \kappa_1\sin\kappa_2(Z'-a)\cos\kappa_1 a]$$

when $Z \in [c]$ and $Z' \in [b]$.

For other regions of Z and Z', the expressions of the Green functions can be found by appropriate permutations. In all cases,

$$\mathrm{Den} = \kappa_1 \cos\kappa_1 a(\sin\kappa_3 c\cos\kappa_2 b + (\kappa_3/\kappa_2)\sin\kappa_2 b\cos\kappa_3 c) - \kappa_2 \sin\kappa_1 a(\sin\kappa_3 c\sin\kappa_2 b - (\kappa_3/\kappa_2)\cos\kappa_2 b\cos\kappa_3 c).$$

In these expressions κ_μ is defined by $\kappa_\mu = (1/\hbar)\sqrt{2m(E - K^2/2m - \Sigma_\mu)}$ for $\mu = 1, 2, 3$. Zeros of the real part of the denominator (Den) define the eigenvalues of the energy of the problem considered.

Ohm's law in the present inhomogeneous media is given as

$$j(Z) = \int \sigma(Z, Z')E(Z)\,\mathrm{d}^3Z'$$

where $j(Z)$ is the current density at point Z and $E(Z')$ the electrical field at point Z' assumed to lie along the x-axis. As was pointed out in [17], the conductivity is a non-local characteristic of the media. The expression of the non-local conductivity $\sigma(Z, Z')$ is given by [16]:

$$\sigma(Z, Z') = \frac{\hbar e^2}{\pi N a_0^4}\sum_K v_{K_x}^2 G_K(Z, Z', \epsilon_F + i0)G_K(Z, Z', \epsilon_F - i0) \tag{4}$$

in which a_0 is the lattice constant, N the number of sites in the plane of the layers, and $v_{K_x} = K_x/m$ the x-component of the electron velocity.

In the in-plane current geometry (CIP), the measured conductivity is given by:

$$\sigma = \frac{1}{D}\int_0^D \int_0^D \mathrm{d}Z\,\mathrm{d}Z'\sigma(Z, Z')$$

where $D = a + b + c$ is the total thickness of the sample. The final expression of this conductivity has been calculated analytically; its expression is given in the appendix. The expression of the magnetoresistance is obtained from the calculation of the conductivity in both the parallel and antiparallel alignment configurations of the magnetizations in the successive ferromagnetic layers. In the next section, we use this analytical expression to investigate the influence of the quantization of electron momentum along the z-axis, the respective role of spin-dependent scattering and spin-dependent potential barriers on the magnetoresistance and the variation of magnetoresistance with thicknesses of the various layers.

4. Results and discussion

4.1. Influence of the quantization of electron momentum along the z-axis

The expression given in the appendix shows that the conductivity and the magnetoresistance of the multilayers oscillate as the thicknesses of the layers are varied. These oscillations are due to the quantization of the z component of conduction-electron momentum. They must be distinguished from the magnetoresistance oscillations observed in coupled multilayers which arise from oscillations in the interlayer coupling [26]. When the thickness of layer μ is varied, the period of these oscillations is equal to π/k_F^μ and their amplitude asymptotically

decreases as $(1/k_F^\mu L^\mu)\exp(-L^\mu/l^\mu)$, where L^μ is the thickness of layer μ and l^μ the mean free path of electrons in this layer. It is interesting to note that the mean free path is the characteristic length associated with the damping of quantum oscillations in the conductivity and magnetoresistance of these multilayers.

In figure 1, we compare the magnetoconductivity of sandwiches calculated from the present theory, which takes into account quantization of electron momentum, and from the theory of [17] in which these oscillations have been neglected. For this comparison, we chose $k_F^1 = k_F^2 = k_F^3 = 1$ Å^{-1} equal for spin-up and spin-down electrons, which means that we do not introduce any potential barrier between layers. For the mean free paths, we take the values determined from fits of experimental data on NiFe a Å/Cu b Å/NiFe c Å/FeMn spin-valve structures [17]: $l_1^\uparrow = l_3^\uparrow = 120$ Å; $l_1^\downarrow = l_3^\downarrow = 13$ Å and $l_2^\uparrow = l_2^\downarrow = 215$ Å. In figure 1, the thicknesses of the various layers are large compared to k_F^{-1} (a varying between 0 and 300 Å, $b = 22$ Å, $c = 50$ Å). At these large thicknesses, the quantum oscillations are almost totally damped ($(k_F L^\mu) \gg 1$). Therefore the results of the two theories are indistinguishable.

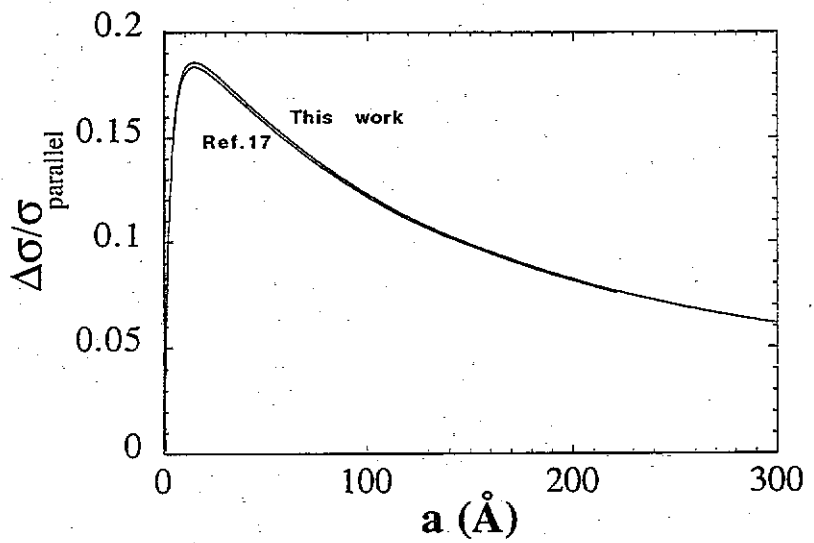

Figure 1. Comparison of magnetoconductivity calculated from the present theory and from [17] for the case of NiFe a Å/Cu 22 Å/NiFe 50 Å/FeMn spin-valve sandwiches for $k_F^1 = k_F^2 = k_F^3 = 1$ Å^{-1} equal for spin-up and spin-down electrons, and $l_1^\uparrow = l_3^\uparrow = 120$ Å; $l_1^\downarrow = l_3^\downarrow = 13$ Å; $l_2^\uparrow = l_2^\downarrow = 215$ Å. The results from the two theories are indistinguishable at these large thicknesses.

In figure 2, we consider a situation with much thinner layers (a varying between 0 and 40 Å, $b = 10$ Å, $c = 10$ Å) and a smaller value of Fermi momentum ($k_F^1 = k_F^2 = k_F^3 = 0.3$ Å^{-1}). In this case, well-defined oscillations are found, the amplitude of which decreases as the thickness of the first layer is increased. We think that it should be possible to observe such oscillations of conductivity and magnetoconductivity in multilayers with very thin layers even in the presence of interfacial roughness provided that this roughness is small compared to the period of oscillations. Fe-based multilayers in which d electrons seem to carry a significant part of the current [24] may be particularly good candidates for the observation of these oscillations. We draw attention to the fact that the oscillations

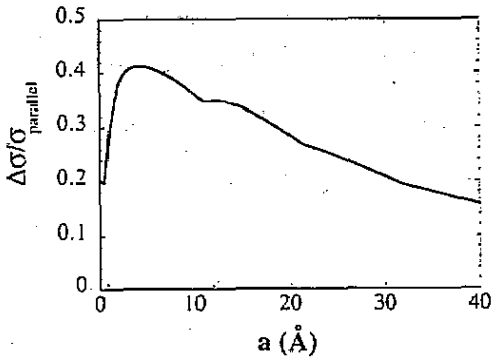

Figure 2. Magnetoconductivity calculated from the present theory in the case of F a Å/NM 10 Å/F 10 Å spin-valve sandwiches for $k_F^1 = k_F^2 = 0.3$ Å^{-1} equal for spin-up and spin-down electrons, and $l_1^\uparrow = l_3^\uparrow = 120$ Å; $l_1^\downarrow = l_3^\downarrow = 13$ Å; $l_2^\uparrow = l_2^\downarrow = 215$ Å. Oscillations are observed in the present theory because of the lower thicknesses and smaller Fermi momenta than those for the case illustrated in figure 1.

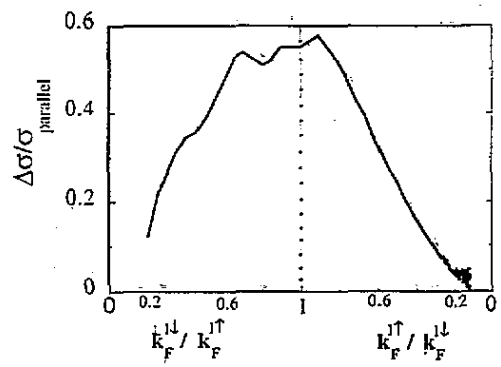

Figure 3. Magnetoconductivity of a sandwich F 10 Å/NM 0 Å/F 10 Å (limit of very thin spacer layer) versus ratio $k_F^{1\downarrow}/k_F^{1\uparrow} (= k_F^{3\downarrow}/k_F^{3\uparrow})$ in the presence of large spin-dependent scattering in the ferromagnetic layers: $l_1^\uparrow/l_1^\downarrow = l_3^\uparrow/l_3^\downarrow = 120$ Å/13 Å; $k_F^{1\downarrow} = k_F^{3\downarrow} = 1$ Å^{-1}.

observed in magneto-optic Kerr rotation, for instance in Fe/Cu multilayers [27], have the same physical origin as the present oscillations in transport properties, namely the quantization of electron momentum in the direction perpendicular to the plane of the layers. However, the Kerr effect is related to transitions within the d-band only, while the transport properties involve both sp and d electrons. Therefore these oscillations are probably more pronounced in magneto-optical than in transport properties. In principle, as in the De Haas Van Alphen effect, the experimental observation of these oscillations might be used to determine Fermi-surface parameters.

4.2. Influence of potential barriers on the giant magnetoresistance

In this section, we successively consider three situations:

(i) the effect of spin-dependent potential barriers in the presence of large spin-dependent scattering;

(ii) the effect of spin-dependent potential barriers when all scattering is not spin-dependent;

(iii) the effect of spin-independent potential barriers in the presence of large spin-dependent scattering.

From this investigation we will show that, in general, the existence of potential barriers (spin-dependent or not) decreases the giant magnetoresistance which mainly originates from spin-dependent scattering. The two effects may have constructive contributions to the magnetoresistance only when spin-dependent scattering is very weak.

4.2.1. The effect of spin-dependent potential barriers in the presence of large spin-dependent scattering. To illustrate this case, we choose the following set of parameters: $l_1^{\uparrow}/l_1^{\downarrow} = l_3^{\uparrow}/l_3^{\downarrow} = 120$ Å/13 Å corresponding to $Ni_{80}Fe_{20}$ [17]; $k_F^{1\downarrow} = k_F^{3\downarrow} = 1$ Å^{-1}; $a = c = 10$ Å, $b = 0$ Å and we vary $k_F^{1\uparrow}$ and $k_F^{3\uparrow}$ keeping $k_F^{1\uparrow} = k_F^{3\uparrow}$. We set $b = 0$ Å (the limit of a very thin spacer layer) to focus on the effect of the spin-dependent barriers at the interfaces between the ferromagnetic layers without additional effects from the spacer layer. The two ferromagnetic layers are assumed identical. In this case, the conduction electrons experience a flat potential when the magnetizations are in parallel alignment and spin-dependent potential barriers when they are in antiparallel alignment. Figure 3 shows the amplitude of the giant magnetoresistance (expressed as the relative change of conductivity normalized by conductivity when the magnetization is in parallel alignment) versus the ratio $k_F^{1\uparrow}/k_F^{1\downarrow}$. The general trend is clearly a decrease in the amplitude of GMR as $|k_F^{1\uparrow} - k_F^{1\downarrow}|$ increases. Some oscillations are observed around this general trend which are due to the quantization of electron momentum along the z-axis as discussed in the preceding section.

4.2.2. The effect of spin-dependent potential barriers in the absence of spin-dependent scattering. We consider here the other limiting case where $l_1^{\uparrow}/l_1^{\downarrow} = l_3^{\uparrow}/l_3^{\downarrow} = 66$ Å/66 Å $= 1$ (the same conductivity as above but without spin-dependent scattering). The other parameters are kept the same as above: $k_F^{1\downarrow} = k_F^{3\downarrow} = 1$ Å^{-1}, $a = c = 10$ Å and $b = 0$ Å. When the ratio $k_F^{1\uparrow}/k_F^{1\downarrow}$ is equal to one, the GMR amplitude is equal to zero as expected in the absence of both spin-dependent scattering and spin-dependent potential barriers. As $k_F^{1\uparrow}/k_F^{1\downarrow}$ is varied above or below unity (see figure 4), an increase of GMR is first observed followed again by a decrease when $|k_F^{1\uparrow} - k_F^{1\downarrow}|$ becomes too large. Such behaviour can be understood in terms of electron reflectance at the potential barriers in the antiparallel magnetic configuration of the sandwich. Indeed, electrons with small angle of incidence are almost ideally reflected with very small penetration length when the height of the potential barriers increases. Therefore for small barrier heights, the GMR arises as a result of the change of conductivity between the two cases without barriers (parallel alignment) and with spin-dependent barriers (antiparallel alignment). However when the barrier height is too large (large or small ratio $k_F^{1\uparrow}/k_F^{1\downarrow}$), these two situations (with or without barriers) become equivalent because the conduction electrons are specularly reflected either on the outer boundaries or on the potential barriers, leading in both cases to the same conductivity (in this case there is no size effect and the two layers are completely decoupled). The maximum amplitude of magnetoresistance that can be obtained from this mechanism of spin-dependent barriers is nevertheless significantly lower than in the case of spin-dependent scattering (compare the amplitudes of the GMR in figures 3 and 4). Therefore, spin-dependent scattering remains the main origin of GMR in magnetic multilayers. Spin-dependent potential barriers can give a constructive contribution to the GMR in the case of very weak spin-dependent scattering. However in most cases, these barriers reduce the

GMR amplitude because they induce a reflection of the conduction electrons and therefore prevent the exchange of electrons between the ferromagnetic layers through the spacer layer. This is the so-called 'channelling effect' also discussed in a classical framework in [14]. The situation would of course be totally different in a geometry with current flowing perpendicular to the plane of the layers (CCP geometry). Work is in progress to treat the case of CCP GMR in the presence of barriers.

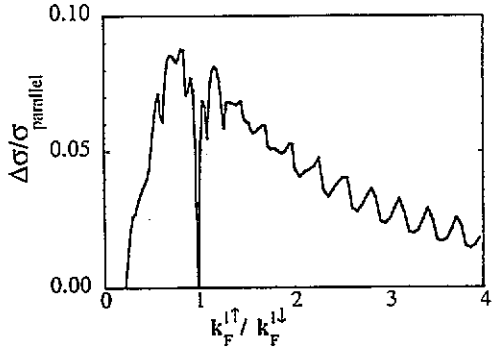

Figure 4. Magnetoconductivity of a sandwich F 10 Å/NM 0 Å/F 10 Å (limit of very thin spacer layer) versus ratio $k_F^{1\downarrow}/k_F^{1\uparrow}(=k_F^{3\downarrow}/k_F^{3\uparrow})$ in the absence of spin-dependent scattering in the ferromagnetic layers: $l_1^{\uparrow}/l_1^{\downarrow}=l_3^{\uparrow}/l_3^{\downarrow}=66$ Å/66 Å $=1$; $k_F^{1\downarrow}=k_F^{3\downarrow}=1$ Å^{-1}.

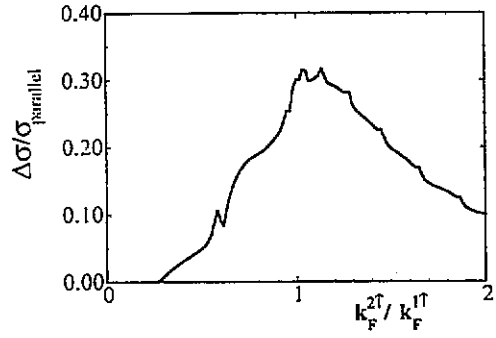

Figure 5. Magnetoconductivity of a sandwich F 10 Å/NM 20 Å/F 10 Å versus ratio $k_F^{2\uparrow}/k_F^{1\uparrow}$ in the presence of large spin-dependent scattering in the ferromagnetic layers: $l_1^{\uparrow}/l_1^{\downarrow}=l_3^{\uparrow}/l_3^{\downarrow}=$ 120 Å/13 Å; $l_2^{\uparrow}=l_2^{\uparrow}=215$ Å; $k_F^{1\downarrow}=k_F^{3\downarrow}=k_F^{1\uparrow}=k_F^{3\uparrow}=0.6$ Å^{-1}.

4.2.3. The effect of spin-independent potential barriers in the presence of spin-dependent scattering. We now consider the situation where potential barriers exist between the spacer layer and the ferromagnetic layers but are not spin dependent. The set of parameters chosen is: $l_1^{\uparrow}/l_1^{\downarrow}=l_3^{\uparrow}/l_3^{\downarrow}=120$ Å/13 Å; $l_2^{\uparrow}/l_2^{\downarrow}=215$ Å/215 Å $=1$; $k_F^{1\uparrow}/k_F^{1\downarrow}=k_F^{3\uparrow}/k_F^{3\downarrow}=0.6/0.6=1$ and we vary $k_F^{2\downarrow}$ in the spacer layer keeping $k_F^{2\downarrow}=k_F^{2\uparrow}$ (non-magnetic spacer). Figure 5 shows the result. The same general trend is observed as in the two previous cases. The GMR amplitude is maximal in the absence of potential barriers and decreases as the height of the barriers increases due to reflection of conduction electrons.

4.3. Influence of the nature and thickness of the spacer layer

In this section, we investigate the effect of the spacer layer on the magnetoresistance of the sandwich. In particular we compare the situations in which the spacer constitutes either a potential barrier or a potential well for conduction electrons.

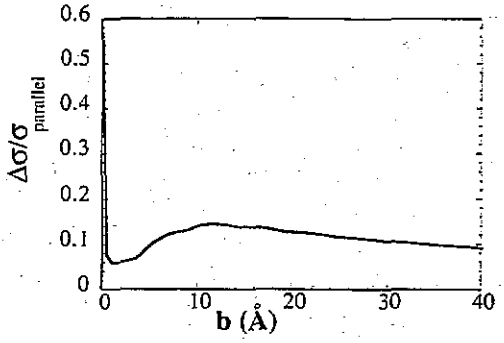

Figure 6. Magnetoconductivity of a sandwich of composition F 5 Å/NM b Å/F 5 Å versus thickness b of the spacer layer (b varying from 0 to 40 Å). The parameters are: $l_1^{\uparrow}/l_1^{\downarrow} = l_3^{\uparrow}/l_3^{\downarrow} = 120$ Å/13 Å; $l_2^{\uparrow}/l_2^{\downarrow} = 215$ Å/215 Å $= 1$; $k_F^{1\uparrow}/k_F^{1\downarrow} = k_F^{3\uparrow}/k_F^{3\downarrow} = 1$ Å^{-1}/1 Å$^{-1} = 1$ and $k_F^{2\uparrow} = k_F^{2\downarrow} = 0.6$ Å^{-1}. The spacer layer constitutes a potential barrier for conduction electrons.

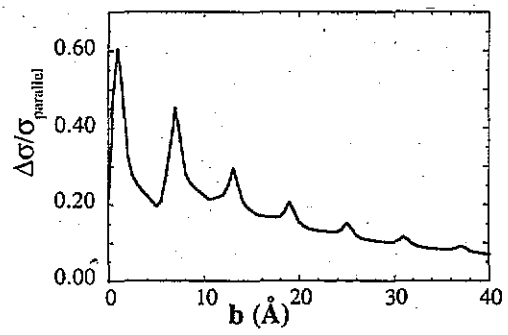

Figure 7. Magnetoconductivity of a sandwich of composition F 5 Å/NM b Å/F 5 Å versus thickness b of the spacer layer (b varying from 0 to 40 Å). The parameters are: $l_1^{\uparrow}/l_1^{\downarrow} = l_3^{\uparrow}/l_3^{\downarrow} = 120$ Å/13 Å; $l_2^{\uparrow}/l_2^{\downarrow} = 215$ Å/215 Å $= 1$; $k_F^{1\uparrow}/k_F^{1\downarrow} = k_F^{3\uparrow}/k_F^{3\downarrow} = 0.3$ Å^{-1}/0.3 Å$^{-1} = 1$ and $k_F^{2\uparrow} = k_F^{2\downarrow} = 0.6$ Å^{-1}. The spacer layer constitutes a potential well for conduction electrons.

Figure 6 represents the magnetoconductivity of a sandwich of composition F 5 Å/NM b Å/F 5 Å versus the thickness b of the spacer layer (b varying from 0 to 40 Å). The parameters are: $l_1^{\uparrow}/l_1^{\downarrow} = l_3^{\uparrow}/l_3^{\downarrow} = 120$ Å/13 Å; $l_2^{\uparrow}/l_2^{\downarrow} = 215$ Å/215 Å $= 1$; $k_F^{1\uparrow}/k_F^{1\downarrow} = k_F^{3\uparrow}/k_F^{3\downarrow} = 1$ Å^{-1}/1 Å$^{-1} = 1$ and $k_F^{2\uparrow} = k_F^{2\downarrow} = 0.6$ Å^{-1}. The smaller value of the Fermi momentum in the spacer layer compared to in the ferromagnetic layers implies that the spacer acts as a potential barrier. A dramatic decrease in the magnetoconductivity is observed as only one monolayer of spacer is introduced between the two ferromagnetic

layers (from 60% to 7%). At larger thicknesses, the magnetoresistance exhibits a smooth maximum modulated by oscillations due to the quantization of momentum along the z-axis. The presence of potential barriers may explain the absence of GMR or its very low amplitude observed in some multilayers. It is indeed striking that Fe/Cr [1] multilayers exhibit a large GMR while only small magnetoresistance has been observed in Fe/Cu multilayers [2]. In contrast Co/Cu or NiFe/Cu multilayers exhibit a very large GMR [2–4] but neither Co/Cr nor NiFe/Cr [28]. Similarly NiFe/Cu/NiFe/FeMn spin-valve sandwiches show large GMR while NiFe/Al/NiFe/FeMn do not exhibit any magnetoresistance [29]. Several reasons can be put forward to explain the puzzling absence of GMR in some of these systems. For instance in NiFe/Al it has been observed that large interdiffusion between Permalloy and aluminium takes place at the interfaces with the formation of an NiFeAl paramagnetic interfacial alloy. This interfacial alloy can provoke strong spin-flip scattering leading to the absence of GMR in this system [29]. In NiFe/Cr multilayers it has been proposed that competing spin-dependent scattering phenomena at the NiFe/Cr interfaces (larger scattering for spin-up electrons) and in the bulk of the NiFe layers (larger scattering for spin-down electrons) may explain the very low magnetoresistance amplitude of these multilayers [28]. However we believe that in all cases the existence of potential barriers resulting from a mismatch of the Fermi wavevectors in the adjacent materials may explain or at least contribute to the very low GMR observed in several of the systems listed above.

Figure 7 illustrates the opposite situation in which the spacer layer constitutes a potential well. We choose here: $l_1^{\uparrow}/l_1^{\downarrow} = l_3^{\uparrow}/l_3^{\downarrow} = 120$ Å/13 Å, $l_2^{\uparrow}/l_2^{\downarrow} = 215$ Å/215 Å $= 1$, $k_F^{1\uparrow}/k_F^{1\downarrow} = k_F^{3\uparrow}/k_F^{3\downarrow} = 0.3$ Å^{-1}/0.3 Å$^{-1} = 1$ and $k_F^{2\uparrow} = k_F^{2\downarrow} = 0.6$ Å^{-1}. The thicknesses of the ferromagnetic layer are the same as in the previous case: $a = c = 5$ Å. The general trend is a smooth decrease of GMR due to the scattering in the spacer layer and to the shunting of the current in this layer. However, well-defined damped oscillations of period $\pi/k_F^{2\uparrow} \approx 5.2$ Å are observed which are again due to the quantization of momentum in the direction perpendicular to the plane of the layers. Therefore the presence of potential wells between the ferromagnetic layers does not affect significantly the GMR amplitude in contrast to potential barriers which drastically reduce the GMR as shown above.

5. Conclusion

We have presented a real-space quantum theory of giant magnetoresistance in magnetic multilayers which takes into account spin-dependent scattering in the ferromagnetic layers and existence of spin-dependent (or not) potential barriers (or wells) between layers. We have shown that the quantization of electron momentum along the direction perpendicular to the plane of the layers leads to well-defined oscillations in conductivity and magnetoresistance which should be observable experimentally. We have demonstrated that the main origin of the giant magnetoresistance in magnetic multilayers remains spin-dependent scattering and that in most cases (except if the spin-dependent scattering is very weak) the existence of potential barriers (even spin-dependent barriers) decreases the GMR amplitude. Therefore in order to obtain large GMR, it seems important to choose couples of magnetic and non-magnetic materials which have good matching of Fermi momentum to minimize the effect of potential barriers.

Acknowledgment

One of us (Professor A Vedyayev) acknowledges Commissariat à l'Energie Atomique for a fellowship thanks to which this work has been possible.

Appendix

In this Appendix, the analytical expression of the conductivity of a sandwich of composition F a Å/NM b Å/F c Å with infinite potential walls on outer boundaries is given. This expression is the sum of nine terms which must be integrated within different intervals. The following notations are used:

$$f(x) = (1-x)/2 \qquad \nu_\mu = k_F^{(1)}/k_F^\mu$$

$$c_\mu = k_F^\mu \left| \mathrm{Re}\left(\sqrt{1-(1-x)\nu_\mu^2 - i/l_\mu k_F^\mu}\right)\right|$$

$$d_\mu = k_F^\mu \left| \mathrm{Im}\left(\sqrt{1-(1-x)\nu_\mu^2 - i/l_\mu k_F^\mu}\right)\right|$$

with $x = 1 - K^2/k_F^{(1)^2}$. l_μ and k_F^μ represent respectively the mean free path and Fermi wave vector of the considered species of electrons (spin-up or spin-down) in layer μ.

$$\begin{aligned}
\text{Term 1} = \{&c_1c_2(1+e^{-4d_1a})\\
&\times[4(c_3/c_2)(1+e^{-4d_2b})(1-e^{-4d_3c}) + 2(c_3^2/c_2^2+1)(1-e^{-4d_2b})(1+e^{-4d_3c})\\
&+ 4e^{-2d_3c}(c_3^2/c_2^2-1)(1-e^{-4d_2b})\cos 2c_3c]\\
&+ (1-e^{-4d_1a})[(1+e^{-4d_2b})(1+e^{-4d_3c})\left(\frac{c_1^2c_3^2}{c_2^2}+c_1^2+c_2^2+c_3^2\right)\\
&+ 2(1-e^{-4d_2b})(1-e^{-4d_3c})(c_1^2c_3/c_2+c_2c_3)\\
&+ 2e^{-2d_2b}(1+e^{-4d_3c})\left(-\frac{c_1^2c_3^2}{c_2^2}+c_1^2-c_2^2+c_3^2\right)\cos 2c_2b\\
&+ 2e^{-2d_3c}(1+e^{-4d_2b})\left(\frac{c_1^2c_3^2}{c_2^2}-c_1^2-c_2^2+c_3^2\right)\cos 2c_3c\\
&+ 8e^{-2d_3c-2d_2b}(c_1^2c_3/c_2-c_2c_3)\sin 2c_3c\sin 2c_2b\\
&+ 4e^{-2d_3c-2d_2b}\left(-\frac{c_1^2c_3^2}{c_2^2}-c_1^2+c_2^2+c_3^2\right)\cos 2c_3c\cos 2c_2b]\}.
\end{aligned}$$

$$\begin{aligned}
\text{Term 2} = \{&(1+e^{-4d_2b})[2(c_3/c_2)(c_1^2+c_2^2)(1-e^{-4d_3c})(1+e^{-4d_1a})\\
&+ 2(c_1/c_2)(c_3^2+c_2^2)(1+e^{-4d_3c})(1-e^{-4d_1a})\\
&+ 4e^{-2d_1a}(1-e^{-4d_3c})(c_3/c_2)(c_1^2-c_2^2)\cos 2c_1a\\
&+ 4e^{-2d_3c}(1-e^{-4d_1a})(c_1/c_2)(c_3^2-c_2^2)\cos 2c_3c] + (1-e^{-4d_2b})\\
&\times[(1+e^{-4d_1a})(1+e^{-4d_3c})(c_1^2/c_2^2+1)(c_2^2+c_3^2)+4c_1c_3(1-e^{-4d_1a})(1-e^{-4d_3c})\\
&+ 2e^{-2d_3c}(1+e^{-4d_1a})(c_1^2/c_2^2+1)(-c_2^2+c_3^2)\cos 2c_3c\\
&+ 2e^{-2d_1a}(1+e^{-4d_3c})(c_1^2/c_2^2-1)(c_2^2+c_3^2)\cos 2c_1a\\
&+ 4e^{-2d_3c-2d_1a}(c_1^2/c_2^2-1)(-c_2^2+c_3^2)\cos 2c_3c\cos 2c_1a]\}.
\end{aligned}$$

Term 3 = Term 1 with permutation $1 \leftrightarrow 3$ and $a \leftrightarrow c$.

$$\begin{aligned}\text{Term 4} = (1-\mathrm{e}^{-4d_3c})[&c_2c_3(1-c_1/c_2)^2(1+\mathrm{e}^{-4d_1a})(1-\mathrm{e}^{-4d_2b})+4c_1c_3(1-\mathrm{e}^{-4d_1a-4d_2b})\\&+2c_2c_3\mathrm{e}^{-2d_1a}(1-\mathrm{e}^{-4d_2b})(c_1^2/c_2^2-1)\cos 2c_1a].\end{aligned}$$

$$\begin{aligned}\text{Term 5} = \{&4c_1c_3(1-\mathrm{e}^{-4d_3c})(1-\mathrm{e}^{-4d_1a})(1-\mathrm{e}^{-2d_2b})^2+(1-\mathrm{e}^{-4d_2b})\\&\times[(1+\mathrm{e}^{-4d_1a})(1-\mathrm{e}^{-4d_3c})c_2c_3(c_1^2/c_2^2+1)+(c_1/c_2)\\&\times(1-\mathrm{e}^{-4d_1a})(1+\mathrm{e}^{-4d_3c})(c_2^2+c_3^2)\\&+2\mathrm{e}^{-2d_3c}(1-\mathrm{e}^{-4d_1a})(c_1/c_2)(-c_2^2+c_3^2)\cos 2c_3c\\&+2\mathrm{e}^{-2d_1a}(1-\mathrm{e}^{-4d_3c})c_2c_3(c_1^2/c_2^2-1)\cos 2c_1a]\}.\end{aligned}$$

Term 6 = Term 4 with permutation $1 \leftrightarrow 3$ and $a \leftrightarrow c$.

$$\begin{aligned}\text{Term 7} = 2(c_1/c_2)(1-\mathrm{e}^{-4d_1a})[&4c_2c_3(1-\mathrm{e}^{-2d_2b})(1-\mathrm{e}^{-4d_3c-2d_2b})\\&+(c_2-c_3)^2(1-\mathrm{e}^{-4d_2b})(1+\mathrm{e}^{-4d_3c})+2(c_3^2-c_2^2)\mathrm{e}^{-2d_3c}(1-\mathrm{e}^{-4d_2b})\cos 2c_3c].\end{aligned}$$

$$\text{Term 8} = 8c_1c_3\mathrm{e}^{-2d_2b}(1-\mathrm{e}^{-4d_1a})(1-\mathrm{e}^{-4d_3c})$$

Term 9 = Term 7 with permutation $1 \leftrightarrow 3$ and $a \leftrightarrow c$.

Furthermore, we define:

$$\begin{aligned}\text{Den} = (c_1^2+c_2^2)\{&(1+\mathrm{e}^{-4d_1a})[2(c_3/c_2)(1-\mathrm{e}^{-4d_2b})(1-\mathrm{e}^{-4d_3c})\\&+(c_3^2/c_2^2+1)(1+\mathrm{e}^{-4d_2b})(1+\mathrm{e}^{-4d_3c})]\\&+2(1-c_3^2/c_2^2)[2\mathrm{e}^{-2d_2b-2d_1a}(1+\mathrm{e}^{-4d_3c})\cos 2c_3c\cos 2c_2b\\&-\mathrm{e}^{-2d_3c}(1+\mathrm{e}^{-4d_1a})(1+\mathrm{e}^{-4d_2b})\cos 2c_3c]\\&-8\mathrm{e}^{-2d_3c-2d_2b-2d_1a}\cos 2c_1a[(c_3^2/c_2^2+1)\cos 2c_3c\cos 2c_2b\\&-2(c_3/c_2)\sin 2c_3c\sin 2c_2b]\}\\&+(c_1^2-c_2^2)\{(1+\mathrm{e}^{-4d_1a})[8(c_3/c_2)\mathrm{e}^{-2d_2b-2d_3c}\sin 2c_3c\sin 2c_2b\\&-4(c_3^2/c_2^2+1)\mathrm{e}^{-2d_2b-2d_3c}\cos 2c_3c\cos 2c_2b]\\&+2(1-c_3^2/c_2^2)[\mathrm{e}^{-2d_2b}(1+\mathrm{e}^{-4d_1a})(1+\mathrm{e}^{-4d_3c})\cos 2c_2b\\&-2\mathrm{e}^{-2d_1a-2d_3c}(1+\mathrm{e}^{-4d_2b})\cos 2c_1a\cos 2c_3c]\\&+2\mathrm{e}^{-2d_1a}\cos 2c_1a[(c_3^2/c_2^2+1)(1+\mathrm{e}^{-4d_2b})(1+\mathrm{e}^{-4d_3c})\\&+2(c_3/c_2)(1-\mathrm{e}^{-4d_2b})(1-\mathrm{e}^{-4d_3c})]\}\\&+2c_1c_2\{(1-\mathrm{e}^{-4d_1a})[2(c_3/c_2)(1+\mathrm{e}^{-4d_2b})(1-\mathrm{e}^{-4d_3c})\\&+(c_3^2/c_2^2+1)(1-\mathrm{e}^{-4d_2b})(1+\mathrm{e}^{-4d_3c})]\\&-2(1-c_3^2/c_2^2)[2\mathrm{e}^{-2d_2b-2d_1a}(1+\mathrm{e}^{-4d_3c})\sin 2c_1a\sin 2c_2b\\&+\mathrm{e}^{-2d_3c}(1-\mathrm{e}^{-4d_1a})(1-\mathrm{e}^{-4d_2b})\cos 2c_3c]+8\mathrm{e}^{-2d_3c-2d_2b-2d_1a}\sin 2c_1a\\&\times[(c_3^2/c_2^2+1)\cos 2c_3c\sin 2c_2b+2c_3/c_2\sin 2c_3c\cos 2c_2b]\}.\end{aligned}$$

Then the three following expressions:

$$\text{expre}_1 = \frac{a}{c_1}\frac{\text{Term 1}}{\text{Den}} f(x)$$

$$\text{expre}_2 = \frac{b}{c_2}\frac{l_2}{l_1}\frac{k_F^{(1)}}{k_F^{(2)}}\frac{\text{Term 2}}{\text{Den}} f(x)$$

$$\text{expre}_3 = \frac{c}{c_3}\frac{l_3}{l_1}\frac{k_F^{(1)}}{k_F^{(3)}}\frac{\text{Term 3}}{\text{Den}} f(x)$$

must be integrated in the intervals $[0, 1]$, $[0, 1-\nu_2^{-2}]$ and $[0, 1-\nu_3^{-2}]$, respectively, as the three quantities:

$$\text{expre}_4 = -\frac{l_1}{k_F^{(1)}}\frac{\text{Term 4}}{\text{Den}} f(x)$$

$$\text{expre}_5 = -\left(\frac{l_2}{k_F^{(2)}}\right)^2 \frac{k_F^{(1)}}{l_1}\frac{\text{Term 5}}{\text{Den}} f(x)$$

$$\text{expre}_6 = -\left(\frac{l_3}{k_F^{(3)}}\right)^2 \frac{k_F^{(1)}}{l_1}\frac{\text{Term 6}}{\text{Den}} f(x).$$

For the three following terms, the intervals of integration are different:

$$\text{expre}_7 = \frac{l_2}{k_F^{(2)}}\frac{\text{Term 7}}{\text{Den}} f(x) \qquad \text{in the interval } [\max(0, 1-\nu_2^{-2}), 1]$$

$$\text{expre}_8 = \frac{l_3}{k_F^{(3)}}\frac{\text{Term 8}}{\text{Den}} f(x) \qquad \text{in the interval } [\max(0, 1-\nu_3^{-2}), 1]$$

$$\text{expre}_9 = \left(\frac{l_3}{k_F^{(3)}}\right)\left(\frac{l_2}{k_F^{(2)}}\right)\left(\frac{k_F^{(1)}}{l_1}\right)\frac{\text{Term 9}}{\text{Den}} f(x) \qquad \text{in the interval } [\max(1-\nu_2^{-2}, 1-\nu_3^{-2}), 1].$$

The conductivity of the sandwich in the parallel or antiparallel magnetic configurations is finally given by:

$$\sigma = \frac{3}{2} D^{-1} \sigma^{(1)} k_F^{(1)} \sum_{i=1}^{9} \int_{\text{low}_i}^{\text{up}_i} \text{expre}_i \, dx.$$

In this formula $\sigma^{(1)}$ represents the conductivity of the species of electron considered (spin up or spin down) in layer 1. Low_i and up_i are the lower and upper limits of integration which are given above for each of the nine terms to be integrated. The variable x is related to the incidence of conduction electrons. The total conductivity is the sum of the conductivity of spin-up and spin-down electrons. The magnetoconductivity is obtained by calculating this total conductivity in both configurations of parallel and antiparallel alignment of the magnetizations in the ferromagnetic layers.

References

[1] Baibich M N, Broto J M, Fert A, Nguyen Van Dau F, Petroff F, Etienne P, Creuzet G, Friederich A and Chazelas J 1988 *Phys. Rev. Lett.* **61** 2472

[2] See, for instance, *Proc. Int. Workshop on Spin-Valve Multilayered Structures (Madrid, 1991)* *Proc. NATO Advanced Res. Workshop on Structure and Magnetic Properties of Systems in Reduced Dimension (Cargèse, France 1992)* NATO Series (New York: Plenum) at press

[3] Mosca D H, Petroff F, Fert A, Schroeder P A, Pratt W P and Loloe R 1991 *J. Magn. Magn. Mater.* **94** L-1

[4] Parkin S S P, Bhadra R and Roche K P 1991 *Phys. Rev. Lett.* **66** 2152

[5] Dupas C, Beauvillain P, Chappert C, Renard J P, Triqui F, Veillet P, Velu E and Renard D 1990 *J. Appl. Phys.* **67** 3061

[6] Shinjo T and Yamamoto H 1990 *J. Phys. Soc. Japan* **59** 3061

[7] Dieny B, Speriosu V S, Parkin S S P, Gurney B A, Wilhoit D R and Mauri D 1991 *Phys. Rev.* B **43** 1297

[8] Dieny B, Speriosu V S, Gurney B A, Parkin S S P, Wilhoit D R, Roche K P, Metin S, Peterson D T and Nadimi S 1991 *J. Magn. Magn. Mater.* **93** 101

[9] Camley R E and Barnas J 1989 *Phys. Rev. Lett.* **63** 664

[10] Barnas J, Fuss A, Camley R E, Grünberg P and Zinn W 1990 *Phys. Rev.* B **42** 8110

[11] Barthélémy A and Fert A 1991 *Phys. Rev.* B **43** 13 124

[12] Dieny B 1992 *Europhys. Lett.* **17** 261; 1992 *J. Phys.: Condens. Matter* **4** 8009

[13] Edwards D M, Muniz R B and Mathon J 1991 *IEEE Trans. Magn.* **MAG-27** 3548

[14] Hood R Q and Falicov L M 1992 *Phys. Rev.* B **46** 8287

[15] Levy P M, Zhang S and Fert A 1990 *Phys. Rev. Lett.* **65** 1643

[16] Zhang S, Levy P M and Fert A 1992 *Phys. Rev.* B **45** 8689

[17] Vedyayev A, Dieny B and Ryzhanova N 1992 *Europhys. Lett.* **19** 329

[18] Levy P M, Shi Z P, Zhang S, Camblong H E and Fry J L 1993 *J. Magn. Magn. Mater.* **121** 357

[19] Itoh H, Inoue J and Maekawa S 1993 *Phys. Rev.* B **47**

[20] Dieny B, Meyer H, Vedyayev A and Ryzhanova N 1993 *J. Magn. Magn. Mater.* **121** 366

[21] Camblong H E and Levy P M 1992 *Phys. Rev. Lett.* **69** 2835

[22] Fert A and Campbell I A 1976 *J. Phys. F: Met. Phys.* **6** 849

[23] Moruzzi V L, Janak J F and Williams A R 1978 *Calculated Electronic Properties of Metals* (New York: Pergamon)

[24] Stearns M B 1973 *Phys. Rev.* B **6** 3326; 1973 *Phys. Rev.* B **8** 4383; 1973 *Phys. Rev.* B **7** 318; 1977 *J. Magn. Magn. Mater.* **5** 167

[25] Brouers F, Vedyayev A and Giorgino M 1973 *Phys. Rev.* B **7** 380

[26] Parkin S S P, More N and Roche K P 1990 *Phys. Rev. Lett.* **64** 2304

[27] Bennett R W, Schwarzacher W and Egelhoff Jr W F 1990 *Phys. Rev. Lett.* **65** 3169

[28] Watson M L, Whiting J S S, Chambers A and Thompson S M 1992 *J. Magn. Magn. Mater.* **113** 97

[29] Dieny B, Speriosu V S, Nozières J P, Gurney B A, Vedyayev A and Ryzhanova N 1993 *Proc. NATO Advanced Res. Workshop on Structure and Magnetic Properties of Systems in Reduced Dimension (Cargèse, France 1992)* NATO Series (New York: Plenum) at press